MICE-NOTE-DET,REC-473 (2015)

Progress on Cherenkov Reconstruction in MICE

Lucien Cremaldi, David Sanders, Don Summers, University of Mississippi - Oxford
Michael Drews, Dan Kaplan, Durga Rajaram, Miles Winter, Illinois Institute of Technology

Abstract

Two beamline Cherenkov detectors (Ckov-a,-b) support particle ID in the MICE beamline. Electrons and high-momentum muons and pions can be identified with good efficiency. We report on the Ckov-a,-b performance in detecting pions and muons with MICE Step I data.

1 Introduction

The international Muon Ionization Cooling Experiment (MICE) [1] is designed to measure muon ionization cooling [2]. Cooling is needed for neutrino factories based on muon decay ($\mu^- \to e^- \,\overline{\nu}_e \,\nu_\mu$ and $\mu^+ \to e^+ \,\nu_e \,\overline{\nu}_\mu$) in storage rings [3] and for muon colliders [4].

The 237 MeV/c data in this note come from runs 3506 to 3509 and 3512 to 3516 taken on 14 and 15 December 2011. The 294 MeV/c data come from runs 4082-4084 taken on 20 May 2012.

The two high density aerogel threshold Cherenkov counters [5], located just after the first time of flight counter, TOF0, in the MICE beamline, are used in support of muon and pion particle identification. The measured [6] refractive indices of the aerogels in the counters are $n_a = 1.069 \pm 0.003$ in Ckov-a and $n_b = 1.112 \pm 0.004$ in Ckov-b. The corresponding momentum thresholds for muons (pions) are at 280.5 (367.9) and 217.9 (285.8) MeV/c, respectively. Light is collected in each counter by four 9354KB eight-inch UV-enhanced phototubes and recorded by CAEN V1731 FADCs (500 MS/s).

A charge integration algorithm identifies charge clusters $q_i, i = 1$–8 in the FADCs where the ADC value crosses a threshold, marking times t_1 and t_2 at the threshold crossings, approximating the pulse beginning and end times. The value of t_{max} at the cluster signal maximum is found. The algorithm integrates the charge within a $t_1 - 8$ ns and $t_2 + 16$ ns timing window in order to ensure full charge collection. The charges are converted to a photoelectron count pe_i, by subtracting a pedestal q_{0i} and then normalizing by the single photoelectron q_{1i} charge for each phototube:

$$pe_i = \frac{q_i - q_{0i}}{q_{1i}}\,, \qquad i = 1 - 8. \tag{1}$$

In the event that no cluster is found, the algorithm repeats an exhaustive search for small ≈1-pe signals. For all $q_i > 0$, the total charge, arrival time, t_1, and t_{max} are stored per event.

The asymptotic β=1 light yield $N_{\beta=1}$ in each counter is measured using the electron peak in MICE calibration-beam runs, giving 25 and 16 photoelectrons (pe's) in Ckov-b and Ckov-a, respectively, for a nominal run. The photoelectron yields versus momentum are displayed in Figure 1. The observed muon thresholds, 213 ± 4 and 272 ± 3 MeV/c, are in reasonable agreement with the expectations given above. The average number of photoelectrons for normal incidence in the counters can be predicted from the Cherenkov angle $\cos\theta_c = 1/n\beta$, and, near threshold $\beta_{th} = 1/n$,

$$N_{pe} = N_{\beta=1} \times \sin^2\theta_c = N_{\beta=1} \times (1 - (p_{th}/p)^2)\,. \tag{2}$$

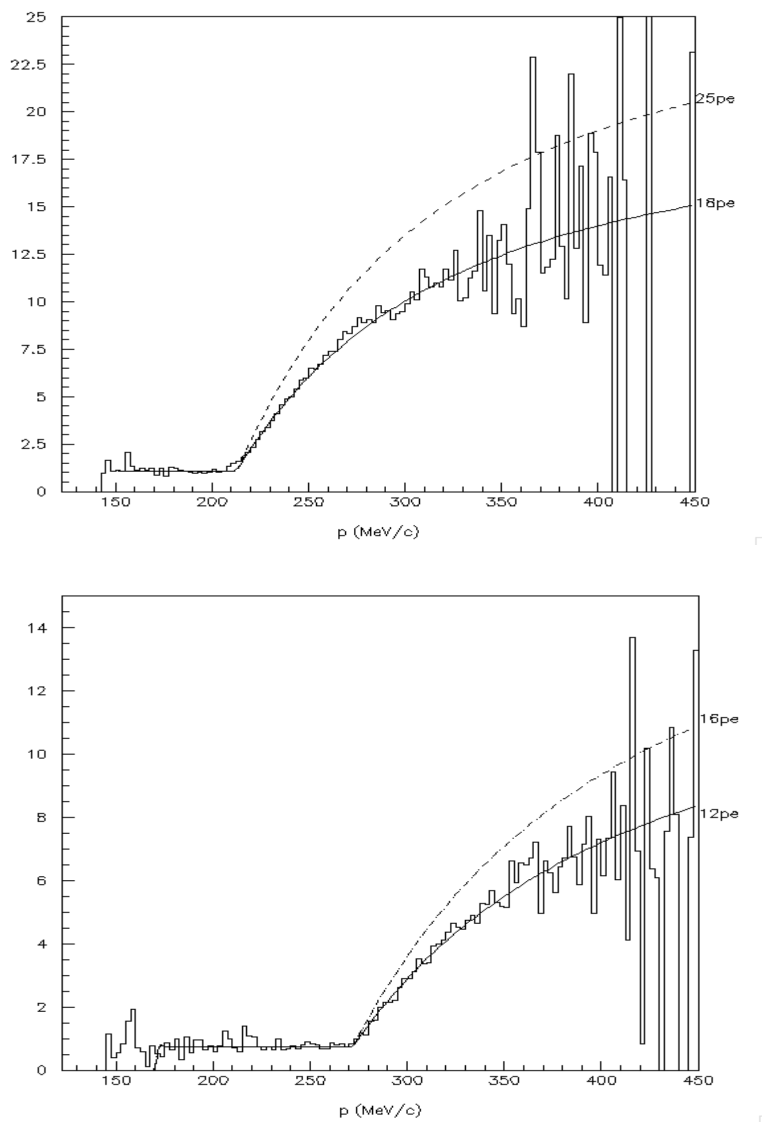

Figure 1: Photoelectron curves versus momentum for muons in Ckov-b (top panel) with the superimposed function $f = 1.1 + 18 \times [1 - (213/p)^2]$, and similarly for muons in Ckov-a (bottom), with $f = 0.75 + 12 \times [1 - (272/p)^2]$. The $N_{\beta=1}$ values are about 75% of the values predicted from the asymptotic photoelectron spectrum of $\beta = 1$ electrons (labeled on the right) — not unexpected since the electrons have a greater likelihood to produce accompanying electrons in TOF0, which acts effectively as a "preshower" radiator.

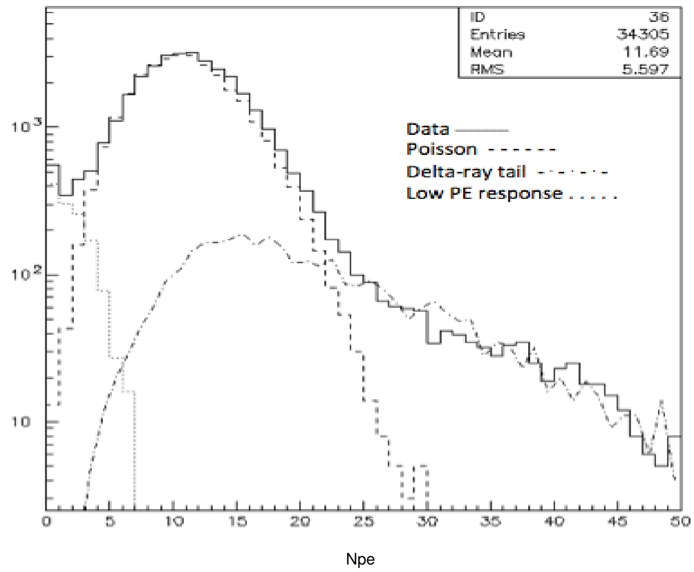

Figure 2: Typical photoelectron spectrum seen for muons or pions above threshold in Ckov-b (solid histogram), together with model fit components: Poisson (dashed), delta-ray tail (dot-dashed), and anomalous low-N_{pe} component (dotted).

As seen in Figure 2, the photoelectron spectra for μ, π are observed to be Poisson-like with tails from electromagnetic showers and delta rays produced as the particle traverses TOF0 and the aerogel radiator. Secondary electrons from these processes above about 1 MeV/c produce Cherenkov light 5–6% of the time for each particle passage. For small-N_{pe} signals, the measured spectra contain more zero-pe events than expected from pure Poisson-like behavior $P_0(x) = e^{-x}$, $x = \langle N_{pe} \rangle$. Based on the data we have parameterized the behavior with the function

$$P_0(x) = \max\left(e^{-x}, 0.2298 e^{-0.34344x}\right). \tag{3}$$

2 Beam Particle Spectra

The D1 and D2 dipoles predominantly control the beam momentum and particle types transmitted through the MICE spectrometer. In the $p_{tgt} \approx p_{D1} \approx p_{D2}$ setting (calibration mode), the beamline transports a mixture of decay/conversion electrons, decay muons, and primary pions. For $p_{tgt} \approx p_{D1} \approx 2p_{D2}$, backward muon decays from the decay solenoid (DS) are selected. G4beamline [7] Monte Carlo runs indicate that a small leakage of primary pions through the D2 selection magnet can occur at the $\sim 1\%$ level. (Note that these pions produce high-momentum decay muons in the MICE beam — a different production mechanism than that of the nominal MICE beam, which comes from pion decays *upstream* of D2.) Both these high-momentum pions and their decay muons should be observable in both Ckov-a and Ckov-b. Ckov-a can be used effectively to select the high-momentum π, μ events that are just over threshold. In Figure 3 we show the MC spectrum of high-momentum pions emerging from the decay solenoid (DS) and then those π (green) and μ (red) that will trigger Ckov-a. The ratio of high-momentum muons to pions is about 5:1 at TOF0. Pions emerging from D2 are badly aimed and most miss the TOF1 trigger hodoscope 7.733

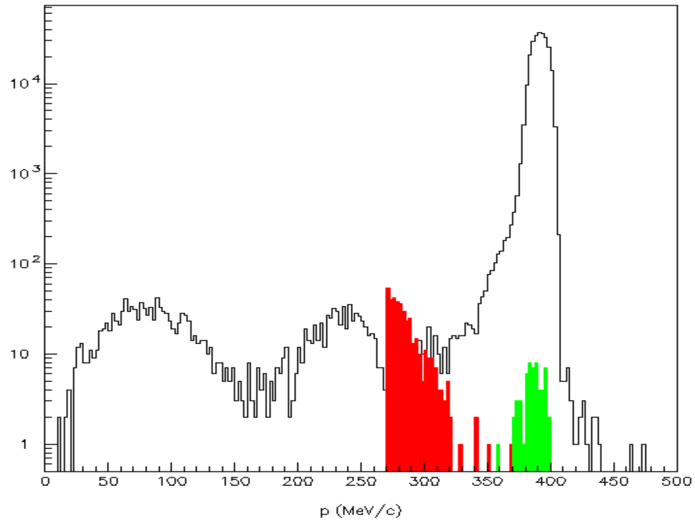

Figure 3: (Solid) MC momentum spectra of pions emerging from the DS: (green) pions surviving at TOF0 with $p \geq 354\,\mathrm{MeV}/c$; (red) muons surviving at TOF0 with $p \geq 270\,\mathrm{MeV}/c$.

meters downstream. At TOF1 the high-momentum-muon to pion ratio given by G4beamline is approximately 20:1.

3 Analysis

For unambiguous identification of particle species the Cherenkov detectors (measuring velocity) would need a momentum measurement from the MICE tracker, which was not available in Step I data. Muons and pions are thus indistinguishable here by the Cherenkov effect. In the following analysis we look for high-momentum π or μ that trigger Ckov-a. An additional cut on the number of photoelectrons in Ckov-b serves to suppress the $\approx 6\%$ of slow "background" events that pass the Ckov-a cut due to delta-ray emission.

We analyzed 120k Step I muon events with $p_{tgt} = 400$ MeV/c and $p_{D2} = 237$ MeV/c (the "standard" muon beam settings). We also analyzed 35k muon events with $p_{tgt} = 500$ MeV/c and $p_{D2} = 294$ MeV/c. The momentum spectra for these two muon data sets are displayed in Figure 4. In Figure 5 we show the time-of-flight spectrum in the standard $p_{D2} = 237$ MeV/c muon running condition. The electron time-of-flight peak is centered at 25.84 ns with a width $\sigma = 0.164$ ns. In the high-momentum time-of-flight window 27 ns $<$ tof $<$ 28 ns a small fraction of particles may be pions.

In Figure 6 we cut away the electron signal (by requiring tof > 26.4 ns) and also make a Ckov-a $N_{pe} > 2$ cut. The shoulder centered at 27.6 ns is made up of fast muons and pions triggering in Ckov-a and at TOF1. The background events centered approximately at tof$\,=28$ ns are from particles with momenta below threshold in Ckov-a, but giving $N_{pe} > 2$ Ckov-a light by delta-ray emission. This background is consistent with the expected 6% contamination level. The tof$\,=27.6$ ns peak corresponds to $p_\mu = 277$ MeV/c or $p_\pi = 363$ MeV/c, both above threshold in Ckov-a.

Fast muons and pions will leave considerable light in Ckov-b. According to Equation 2 about 10 pe will be produced in Ckov-b at $p_\mu = 270$ MeV/c. The probability for simultaneous delta-ray

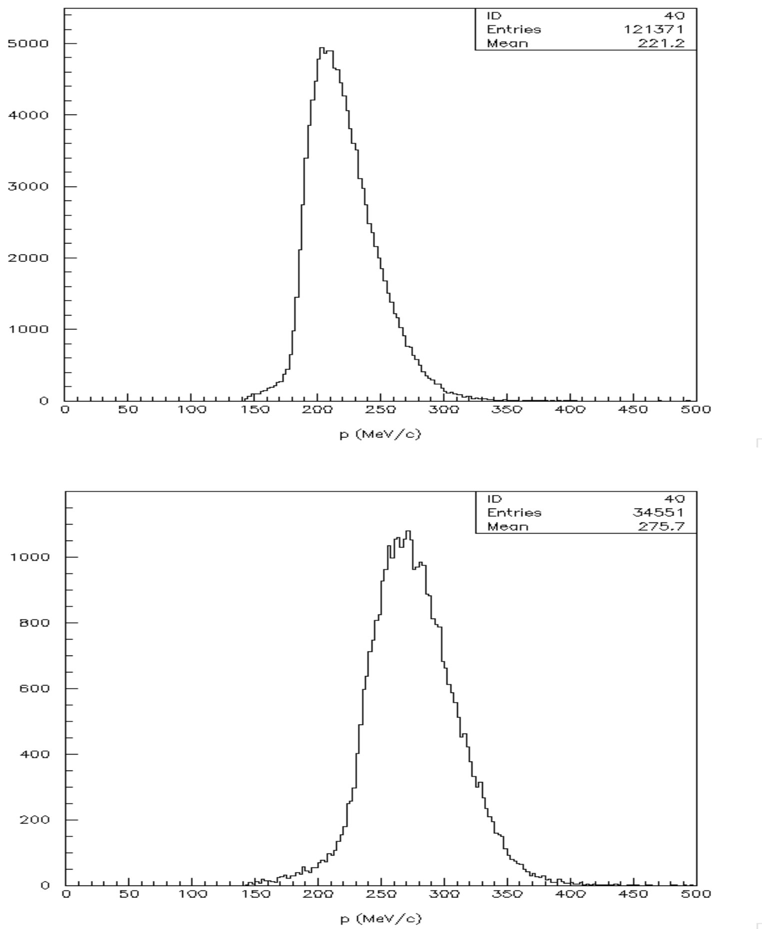

Figure 4: Momentum spectra determined for $p_{D2} = 237$ MeV/c data (top) and $p_{D2} = 294$ MeV/c data (bottom). Momenta were determined from time-of-flight, $\Delta t = L/c\sqrt{1 + (m/p)^2}$, assuming particles are muons.

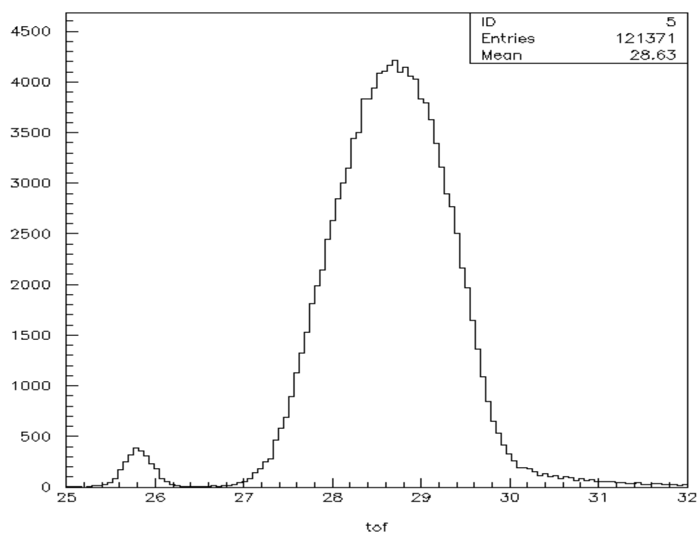

Figure 5: Time-of-flight spectrum from standard (p_{D2} = 237 MeV/c) muon runs. The electron time-of-flight peaks just below 26 ns.

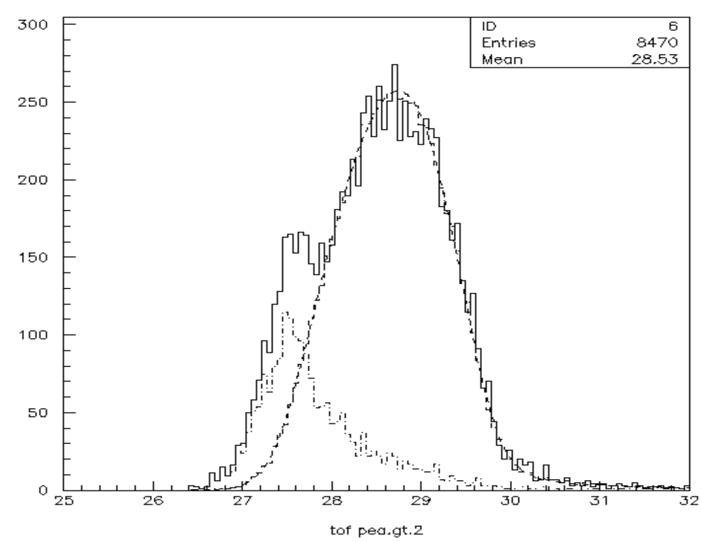

Figure 6: Time-of-flight spectrum with pea>2 cut (solid) with shape of muon spectrum superimposed(dashed). Fast π-μ are identified as the satellite peak centered at 27.6 ns. A cut on peb>8 (dot-dash) further reduces the delta-ray background.

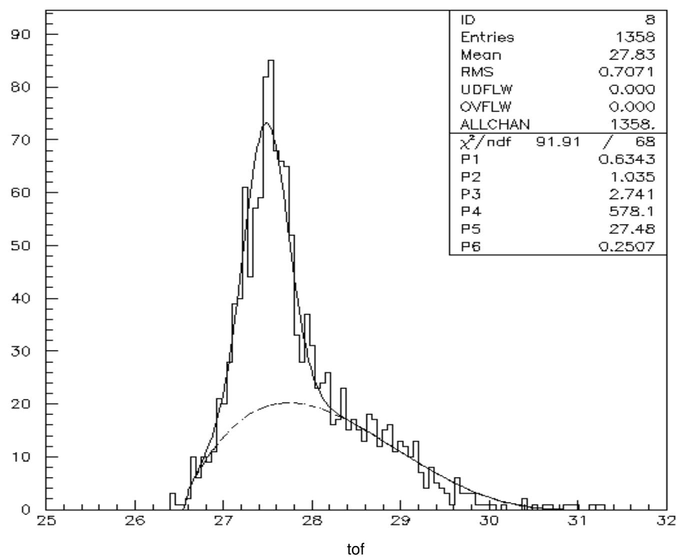

Figure 7: Time-of-flight spectrum with pea$>$ 2 and peb$>$ 10 cuts, greatly reducing the delta-ray contribution.

detection in *both* Ckov-a *and* Ckov-b will be about $0.06^2 = 3.6 \times 10^{-3}$. In Figure 7 we add a Ckov-b $N_{pe} > 10$ cut. The delta-ray background is substantially reduced to about 500 events. A fit to Gaussian signal and phase-space background of the form ($x \equiv$ time of flight)

$$f = \frac{N}{\sqrt{2\pi}\sigma} e^{-(x-\bar{x}^2)/2\sigma^2} + B\ (x - x_{lo})^\alpha (x_{hi} - x)^\beta \tag{4}$$

gives 539 ± 34 signal events. When corrected for efficiency (see Section 4) we obtain $N = 1002 \pm 56$ events. By varying the fitting parameters we find a ± 101-event systematic (syst) uncertainty (discussed in Section 5). The fast π-μ fraction is thus

$$R_{\mu\pi} = \frac{1002 \pm 56 \pm 101}{118,793} = [0.84 \pm 0.05\,(\text{stat}) \pm 0.09\,(\text{syst})]\%\,. \tag{5}$$

If we assume all fast π-μ are pions, we can obtain upper limits on the pion fraction: $R_{\mu\pi} < 0.97\%$ (90% CL) and $R_{\mu\pi} < 1.00\%$ (95% CL). Any Bayesian model [8] would require some prior knowledge of the pion-to-muon ratio in the beam. Estimating this (based on the G4beamline simulation) to be about 1/20 (or about 50 pions) allows us to estimate the fraction of pions in the beam to be $\pi/\mu \simeq 50/119,000 = 0.04\%$.

4 Efficiency Correction

For the efficiency correction we use the $p_{D2} = 294$ MeV/c data set. The muons in this data set span the Ckov-b and Ckov-a muon thresholds well at 212 MeV/c and 272 MeV/c respectively (see Figure 4(bottom)). We assume the corresponding pion efficiency behaves in a similar manner. This assumption will be checked with π-μ-e calibration data (Section 5). The efficiency curves for Ckov-a(b), $\epsilon_{a(b)}(\Delta t)_i$ in each tof bin are determined by taking the ratio of the number of events n_i

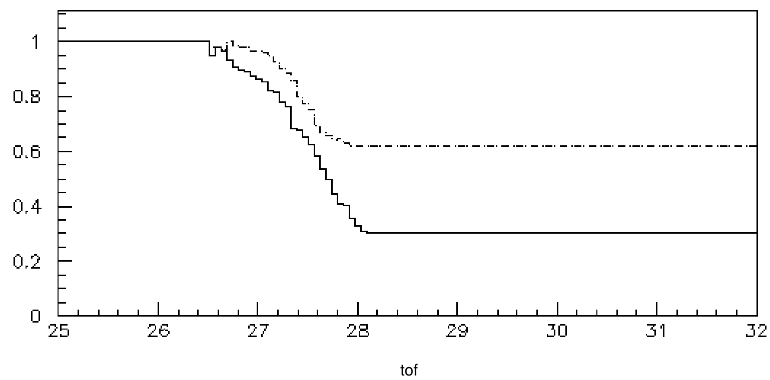

Figure 8: Efficiency curves $\epsilon_{a(b)}$ vs tof (in ns), in Ckov-b with pea>10 (solid) and Ckov-a, peb>2 (dashed).

satisfying the pea(b)$>x$ cut in the i^{th} tof bin to the total number of events N_i in that tof bin with no Ckov cut applied:

$$\epsilon_{a(b)}(\Delta t)_i = n_i(\text{pea} > x)/N_i\,, \qquad x = 2(10)\,\text{pe}\,. \tag{6}$$

The efficiency curves are displayed in Figure 8. Below 26.5 ns and above 28.0 ns, where data are sparse, asymptotic averages were used.

5 Systematic Errors

The systematic errors on the measurement are dominated by the signal fit, and also the efficiency correction $1/\epsilon_a\epsilon_b$ for Ckov-a and Ckov-b. The efficiency corrections were compared with efficiency corrections from π-μ-e calibration data where muons and pions can be identified via time-of-flight. The average efficiency shift between the π-μ-e calibration data and the $p_{D2} = 294$ MeV/c muon data sets gave systematic error shifts of $\pm0.7\%$ and $\pm3.4\%$ (a,b) on the $n = 1002$ fitted π-μ events, or ±7 and ±34 events respectively. Taken in quadrature we obtain a ±35 event systematic error on the efficiency correction. For the fit correction we varied the signal and background fits and determined ±95 event count error in Equation 5 corresponding to 0.08% absolute error. When taken in quadrature, we obtain a ±101 event systematic error on the π-μ signal.

Table 1: Systematic error estimates on the number of fitted π-μ events.

Systematic error	% error	# events	Source
Efficiency correction Ckov-a	0.7%	7	comparison to muon calibration runs
Efficiency correction Ckov-b	3.4%	34	comparison to muon calibration runs
Fitting model	9.4%	95	variation of fit parameters

6 Conclusion

We have used the Ckov-a,-b counters to measure the fast-π-or-μ fraction in Step I data. Under the assumption that fast π-μ's dominate the pion background (Figure 3), we measure the fast π-μ ratio to be $R_{\mu\pi} < 0.97\%$ (90% CL) and $R_{\mu\pi} < 1.00\%$ (95% CL). Under the further assumption from MC studies that only 5% of the pions in the fast π-μ beam reach the TOF1 trigger, then the pion contamination level is $\approx 0.04\%$, indeed very small.

References

[1] M. Bogomilov et al., JINST **7** (2012) P05009;
D. Adams et al., Eur. Phys. J. **C73** (2013) 2582;
D. Adams et al., arXiv:1510.08306;
M. Bogomilov et al., arXiv:1511.00556.

[2] D. Neuffer, arXiv:1312.1266;
D. Neuffer, AIP Conf. Proc. **441** (1998) 270;
R. B. Palmer et al., Phys. Rev. ST Accel Beams **8** (2005) 061003;
P. Snopok et al., Int. J. Mod. Phys. **A24** (2009) 987;
J. C. Gallardo and M. S. Zisman, AIP Conf Proc. **1222** (2010) 308;
M. Chung et al., Phys. Rev. Lett. **111** (2013) 184802;
C. Yoshikawa et al., IPAC-2014-TUPME016;
D. Stratakis and R. B. Palmer, Phys. Rev. ST Accel. Beams **18** (2015) 031003;
J. G. Acosta et al., COOL-2015-MOPF07.

[3] D. G. Koshkarev, CERN-ISR-DI-74-62 (1974);
D. Cline and D. Neuffer, AIP Conf. Proc. **68** (1980) 856;
D. Neuffer, IEEE Trans. Nucl. Sci. **28** (1981) 2034;
S. Ozaki, R. B. Palmer, M. S. Zisman et al., BNL-52623 (2001);
M. M. Alsharo'a et al., Phys. Rev. ST Accel. Beams **6** (2003) 081001;
S. Choubey et al., arXiv:1112.2853;
D. Adey et al., Phys. Rev. **D80** (2014) 071301.

[4] C. M. Ankenbrandt et al., Phys. Rev. ST Accel. Beams **2** (1998) 081001;
J. G. Gallardo et al., Snowmass 1996, BNL-52503;
R. B. Palmer et al., Nucl. Phys. Proc. Suppl. **51A** (1996) 61;
D. Neuffer and R. Palmer, Conf. Proc. C940627 (1995) 52;
A. V. Tollestrup, Conf. Proc. C9610311 (1996) 221;
A. M. Sessler, Phys. Today **51N3** (1998) 48.

[5] L. Cremaldi et al., IEEE Trans. Nucl. Sci. **56** (2009) 1475;
D. A. Sanders, Conf. Proc. C090504 (2009) 1696.

[6] L. Cremaldi *et al.*, "Examination of Matsushita High Density Aerogel," MICE-NOTE-149, Sept. 2006, `http://mice.iit.edu/micenotes/public/pdf/MICE0149/MICE0149.pdf`.

[7] T. J. Roberts et al., Conf. Proc. C0806233 (2008) WEPP120.

[8] T. Bayes, Phil. Trans. Roy. Soc. Lond. **53** (1764) 370.